

CLINOATACAMITE, A NEW POLYMORPH OF $\text{Cu}_2(\text{OH})_3\text{Cl}$, AND ITS RELATIONSHIP TO PARATACAMITE AND "ANARAKITE"*

JOHN L. JAMBOR

Department of Earth Sciences, University of Waterloo, Waterloo, Ontario N2L 3G1

JOHN E. DUTRIZAC

CANMET, Department of Natural Resources Canada, 555 Booth Street, Ottawa, Ontario K1A 0G1

ANDREW C. ROBERTS

Geological Survey of Canada, 601 Booth Street, Ottawa, Ontario K1A 0E8

JOEL D. GRICE

Research Division, Canadian Museum of Nature, Ottawa, Ontario K1P 6P4

JAN T. SZYMAŃSKI

CANMET, Department of Natural Resources Canada, 555 Booth Street, Ottawa, Ontario K1A 0G1

ABSTRACT

The new mineral clinoatacamite is a polymorph of $\text{Cu}_2(\text{OH})_3\text{Cl}$: others are botallackite (monoclinic), atacamite (orthorhombic), and possibly paratacamite (rhombohedral). Clinoatacamite is monoclinic, space group $P2_1/n$, a 6.157(2), b 6.814(3), c 9.104(5) Å, β 99.65(4)°, which is transformable to a pseudorhombohedral cell approximating that of paratacamite. Clinoatacamite has been found in specimens from several localities, and coexists with paratacamite in the holotype specimen of paratacamite. The two minerals are not readily distinguished except by optical and X-ray methods: paratacamite is uniaxial negative, whereas clinoatacamite is biaxial negative, $2V_{\text{mes}}$ 75(5)°. Strongest lines of the X-ray powder pattern of clinoatacamite [d in Å(l)(hkl)] are 5.47(100)($\bar{1}01,011$), 2.887(40)($\bar{1}21,\bar{1}03$), 2.767(60)($\bar{2}11$), 2.742(70)(013,202), 2.266(60)(220), 2.243(50)(004), and 1.704(50)($\bar{2}24,040$). Clinoatacamite is readily synthesized, and a series of experiments was conducted to promote the uptake of Zn and duplicate the formula of the dubious mineral "anarakite" ($\text{Cu,Zn})_2(\text{OH})_3\text{Cl}$. Generally, products with more than about 6 mol% Zn proved to be hexagonal, *i.e.*, zincian paratacamite, as did specimens of "anarakite" from the type locality. Holotype paratacamite contains 2–3 wt.% Zn, and it seems that replacement of Cu by small amounts of another cation, such as Ni or Zn, is either favorable or essential to stabilize the rhombohedral (paratacamite) structure. The Powder Diffraction File standard for paratacamite (25–1427) is that of clinoatacamite rather than paratacamite.

Keywords: clinoatacamite, new mineral species, paratacamite, anarakite, $\text{Cu}_2(\text{OH})_3\text{Cl}$ polymorphs, synthesis, Zn–Ni–Co substitutions, X-ray data.

SOMMAIRE

La nouvelle espèce minérale *clinoatacamite* est un polymorphe de $\text{Cu}_2(\text{OH})_3\text{Cl}$, les autres étant botallackite (monoclinique), atacamite (orthorhombique), et possiblement paratacamite (rhomboédrique). La clinoatacamite est monoclinique, groupe spatial $P2_1/n$, a 6.157(2), b 6.814(3), c 9.104(5) Å, β 99.65(4)°, une maille qui est transformable en une autre, pseudorhomboédrique, approximativement celle de la paratacamite. Nous avons trouvé la clinoatacamite à plusieurs endroits; elle coexiste avec paratacamite dans le spécimen holotype de cette dernière. Les deux minéraux ne sont pas facilement différenciables, sauf par méthodes optiques et par diffraction X: la paratacamite est uniaxe négative, tandis que la clinoatacamite est biaxe négative, $2V_{\text{mes}}$ 75(5)°. Les raies les plus intenses du cliché de diffraction X de la clinoatacamite, méthode des poudres [d en Å(l)(hkl)] sont: 5.47(100)($\bar{1}01,011$), 2.887(40)($\bar{1}21,\bar{1}03$), 2.767(60)($\bar{2}11$), 2.742(70)(013,202), 2.266(60)(220), 2.243(50)(004), et 1.704(50)($\bar{2}24,040$). Il est facile de synthétiser la clinoatacamite; nous avons effectué une série de synthèses pour étudier l'incorporation du Zn et évaluer la formule d'une espèce dont le statut est encore douteux, "l'anarakite", de stoechiométrie

* Geological Survey of Canada contribution number 21695.

(Cu,Zn)₂(OH)₃Cl. En général, les produits de synthèse contenant plus de 6% de Zn (base molaire) sont hexagonaux, c'est-à-dire une paratacamite zincifère, tout comme les échantillons "d'anarakite" provenant de la localité type. La paratacamite holotypique contient de 2 à 3% (poids) de Zn, et il semble que l'incorporation de petites quantités d'un autre cation, comme Ni ou Zn, soit favorable ou essentielle à la stabilisation de la structure rhomboédrique de la paratacamite. Le spectre de diffraction X que l'on attribue à la paratacamite dans le fichier de spectres de diffraction, méthode des poudres (fiche 25-1427) est en fait celui de la clinooatcamite.

(Traduit par la Rédaction)

Mots-clés: clinooatcamite, nouvelle espèce minérale, paratacamite, "anarakite", polymorphes de Cu₂(OH)₃Cl, synthèse, substitutions Zn-Ni-Co, données de diffraction X.

INTRODUCTION

Cu₂(OH)₃Cl has been considered to exist as the trimorphous minerals atacamite (orthorhombic), paratacamite (rhombohedral), and botallackite (monoclinic), the crystal structures of which have been described by Wells (1949), Fleet (1975), and Hawthorne (1985), respectively. In addition to these well-characterized minerals, a synthetic phase assigned the same formula was described by Oswald & Guenter (1971) as paratacamite, and is recorded as paratacamite in the Powder Diffraction File (PDF 25-1427); this synthetic phase, however, has a monoclinic cell rather than the rhombohedral cell ascribed to paratacamite by Frondel (1950) and Fleet (1975).

To the distinct Cu₂(OH)₃Cl polymorphs, two of which are monoclinic, should be added "anarakite" (Cu,Zn)₂(OH)₃Cl, which was described by Adib & Ottemann (1972) as a new mineral from the Anarak Province, Iran. They recognized the similarity to paratacamite, but obtained a monoclinic cell different from those known for Cu₂(OH)₃Cl. In his abstract of the data for anarakite, Fleischer (1973) indicated the mineral to be "probably = zincian paratacamite", and subsequently the status was relegated to that of a discredited mineral (e.g., Nickel & Mandarino 1987).

The X-ray powder-diffraction pattern of "anarakite" (PDF 25-325) is similar to that for rhombohedral paratacamite (Frondel 1950; PDF 19-389), but there are slight differences from the data for the monoclinic synthetic phase as reported by Oswald & Guenter (1971; PDF 25-1427). Others who have investigated paratacamite and the Cu₂(OH)₃Cl polymorphs (e.g., Frondel 1950, Sharkey & Lewin 1971, Woods & Garrels 1986, Pollard *et al.* 1989) presumably have attributed these slight variations to the different recording techniques that have been used (e.g., Debye-Scherrer and Guinier), or to the substitutional effects of Zn in anarakite. Visual comparison of Debye-Scherrer films of (Cu,Zn)₂(OH)₃Cl from Anarak and synthetic Cu₂(OH)₃Cl prepared in our laboratory also showed the patterns to be slightly different; this study was undertaken to resolve the observed differences, which intuitively did not seem to be in accord with the effects of Zn-for-Cu substitution.

PARATACAMITE

Paratacamite is rhombohedral. The unit cell has been determined by single-crystal X-ray methods by Frondel (1950), Fleet (1975), and Pring *et al.* (1987). Fleet's (1975) crystal-structure study showed that the mineral has a pronounced subcell with $a' = a/2$, $c' = c$, apparent space-group $R\bar{3}m$. The superstructure is developed by an ordered arrangement of the substructure, and results in the space group $R\bar{3}$ for the full cell with a 13.65, c 14.04 Å. The superstructure dimensions were also obtained by Frondel (1950) and Pring *et al.* (1987).

"ANARAKITE"

The specimens examined in this study are from the type locality of "anarakite", the Kali Kafi mine, Anarak Province, Iran. The specimen studied in the most detail is from the Pinch collection (Pinch #508), now part of the National Mineral Collection housed at the Canadian Museum of Nature, Ottawa, but material similar in appearance was obtained from the Royal Ontario Museum, Toronto (M 35449), and the National Mineral Collection housed at the Geological Survey of Canada, Ottawa (NMC 14654); all samples have aggregates of small emerald-green crystals sprinkled on a distinctively ochreous-colored, thoroughly oxidized, limonite-pervaded porous matrix.

In their original description of "anarakite", Adib & Ottemann (1972) reported the composition to be Cu 48.53, Zn 10.64, Cl 17.25, OH (by difference) 23.58 wt.%. On the basis of Cu + Zn = 2, the results correspond to (Cu_{1.69}Zn_{0.35})(OH)_{2.99}Cl_{1.05}. Electron-microprobe analysis of grains from the Pinch specimen, mounted in polished section, gave a range of compositions: Cu 48.9-53.7, Zn 4.2-8.7, Cl 16.0-16.3 wt.%. The most Zn-rich composition corresponds to (Cu_{1.70}Zn_{0.30})(OH)_{2.98}Cl_{1.02}, and the composition poorest in Zn is (Cu_{1.86}Zn_{0.14})(OH)_{2.99}Cl_{1.01}. Debye-Scherrer X-ray patterns of the material are sharp and were considered at the initiation of our study to be in fairly good agreement with the data given by Adib & Ottemann (1972) for "anarakite" (Table 1). A Guinier - de Wolff pattern taken with Co X-radiation

TABLE 1. X-RAY POWDER DATA FOR ANARAKITE, ZINCIAN PARATACAMITE, AND CLINOATACAMITE

Anarakite (Adib & Ottemann 1972)				Zincian Paratacamite (this study) ²				Clinoatacamite (this study) ³			
<i>I</i> _{est}	<i>d</i> _{meas}	<i>d</i> _{calc} ¹	<i>hkl</i>	<i>I</i> _{est}	<i>d</i> _{meas}	<i>d</i> _{calc}	<i>hkl</i>	<i>I</i> _{est}	<i>d</i> _{meas}	<i>d</i> _{calc}	<i>hkl</i>
65	5.476	5.483	200	100	5.48	5.45	101	100	5.47	5.47	$\bar{1}01,011$
								<5	5.03		
15	4.697	4.682	002	40	4.69	4.68	003	30	4.68	4.68	101
				5	4.52	4.52	012	<5	4.54	4.53	110
10	3.429	3.430	$\bar{3}11$	15	3.424	3.416	110	20	3.406	3.409,3.407	112,020
				<5	3.019	3.019	104	40	2.887	2.892,2.882	$\bar{1}21,103$
20	2.901	2.899	220	30	2.896	2.895	021	60	2.767	2.771	11
100	2.755	2.759	022	75	2.759	2.759	113	70	2.742	2.739,2.736	013,202
15	2.739	2.741	400	20	2.726	2.726	202	10	2.713*	2.714	022
				10	2.343	2.340	006	20	2.339*	2.339	202
10	2.342	2.344	$\bar{1}14$	65	2.263	2.262	024	60	2.266*	2.266	220
70	2.263	2.265	222					50	2.243*	2.244	004
				<5	2.210	2.209	211	5	2.208	2.209	213
10	2.215	2.215	$\bar{4}22$	10	2.035	2.037	205	5	2.045*	2.049	301
10	2.042	2.044	402					10	2.027*	2.027	123
10	2.035	2.031	114	<5	1.930	1.931	116			1.940	310
				10	1.901	1.900	107	5	1.907*	1.906	301
15	1.904	1.902	204					10	1.895*	1.894	213
				25	1.817	1.817	033	20	1.817*	1.818	231
20	1.824	1.828	600	<5	1.751	1.749	125	10	1.807	1.809,1.806	033,105
20	1.817	1.819	333	35	1.708	1.708	220			1.748	231
				<5	1.661	1.660	027	50	1.704	1.705,1.704	224,040
30	1.708	1.708	040	5	1.630	1.630	131	<5	1.664	1.664	321
				<5	1.601	1.604	223	5	1.626	1.628	223
				7	1.509	1.509	208			1.601,1.600	141,314
10	1.514	1.515	602					5	1.516*	1.518,1.517	400,402
				10	1.494	1.493	217	10	1.504*	1.503,1.501	224,411
15	1.496		043	<5	1.471	1.471	401	10	1.487	1.489,1.484	233,125
				5	1.447	1.447	042	5	1.471	1.471,1.467	305,143
				5	1.420	1.419	119	5	1.445	1.447,1.446	241,242
10	1.384		622	15	1.380	1.380	226				
								10	1.387*	1.386	$\bar{4}22$
				10	1.362	1.363	404	5	1.377*	1.377	242
				5	1.350	1.351	321	10	1.368	1.370,1.368	026,404
				<5	1.311	1.308	045	5	1.356*	1.357	044
				10	1.270	1.269	0.2.10	<5	1.346	1.348,1.347	234,051
				15	1.244	1.245	143				
								10	1.271*	1.271	422
								5	1.260*	1.261,1.260	206,017

¹*d*_{calc} values added to the data of Adib & Ottemann, using their monoclinic cell: *a* 11.901, *b* 6.830, *c* 10.162 Å, β 112.87°.

²Zincian paratacamite results obtained from 114.54-mm Gandolfi film (Co radiation); indexed with hexagonal cell *a* 6.832, *c* 14.042 Å for CoKα radiation (λ 1.7890 Å). Specimen from Kali Kafi mine, Anarak Province, Iran. Refinement based on 27 diffraction lines between 3.424 and 1.104 Å for which unambiguous indexing was possible.

³Clinoatacamite from Chuquicamata, Chile (M32176); 114.54-mm Debye-Scherrer pattern, CoKα, indexed with *a* 6.157, *b* 6.814, *c* 9.104 Å, β 99.65°. Diffraction lines with an asterisk were used for the unit-cell refinement. Line at 5.03 is assumed to be due to atacamite.

showed no broadening or multiple-line diffraction effects from Cu–Zn variation in a bulk sample. Two inferences emerged from these results: (a) what we considered to be the “anarakite-type” X-ray powder pattern persists at relatively low Zn contents (less than half that reported in the original paper), and (b) the differences in our powder patterns of “anarakite” and synthetic “paratacamite” (PDF 23–947, 25–1427) are not the result of progressive shifts in diffraction lines, such as may occur in a solid-solution series.

Single-crystal X-ray study of a minute fragment of the Pinch “anarakite”, mounted about *c**, gave a hexagonal cell with cell dimensions subsequently

refined to *a* 6.832, *c* 14.042 Å (Table 1). Although the precession photographs showed no evidence of the strong supercell that is typically present in paratacamite, *i.e.*, *a* = 2*a*', a 90-hour cone-axis photograph along [100] confirmed the presence of the supercell. The weakness of reflections attributed to the supercell suggests that the ordered arrangement of the substructure may be affected by the substitution of Zn for Cu; nevertheless, the unit cell of the Anarak mineral is clearly that of a zincian rhombohedral paratacamite rather than that of the monoclinic mineral described by Adib & Ottemann (1972).

As was stated above, the X-ray powder data for our

TABLE 2. COMPARISON OF THE UNIT CELLS OF ANARAKITE AND SYNTHETIC $\text{Cu}_2(\text{OH})_3\text{Cl}$

	$(\text{Cu,Zn})_2(\text{OH})_3\text{Cl}$ anarakite ¹	$\text{Cu}_2(\text{OH})_3\text{Cl}$ synthetic ²	synthetic, transformed ³
<i>a</i> (Å)	11.901	11.83	11.83
<i>b</i> (Å)	6.830	6.822	6.822
<i>c</i> (Å)	10.162	6.166	10.103
β°	112.87	130.62	112.102

¹Adib & Ottemann (1972), Anarak, Iran²Oswald & Guenter (1971)³Parameters of the Oswald & Guenter (1971) cell after using the transformation of Kracher & Pertlik (1983)

zincian paratacamite and that of "anarakite" (Adib & Ottemann 1972) are in fairly good agreement, and the several additional weaker lines recorded here for the pattern of zincian paratacamite (Table 1) can be satisfactorily indexed with the monoclinic cell of Adib & Ottemann. The major difference between the two patterns is the appearance of split lines at *d* values of 2.042–2.035 and 1.824–1.817 Å in the published pattern of "anarakite", and these splits are adequately indexed only with the monoclinic cell. In their study of Zn-rich paratacamite, Kracher & Pertlik (1983) reported that they were unable to obtain the original specimen of "anarakite", but they noted that the unit cell of "anarakite" can be transformed to that of the monoclinic phase of $\text{Cu}_2(\text{OH})_3\text{Cl}$ synthesized by Oswald & Guenter (1971). The Oswald & Guenter (1971) phase has *a* 11.83, *b* 6.822, *c* 6.166 Å, β 130.62°, and application of the Kracher & Pertlik (1983) transformation $-1\ 0\ 0/0\ -1\ 0/1\ 0\ 2$ gives a unit cell close to that of anarakite (Table 2).

In summary, our results indicated that the zincian paratacamite from Anarak is rhombohedral, and only the weakness of the supercell reflections distinguishes it from previously reported rhombohedral paratacamite. Thus, the monoclinic cell reported by Adib & Ottemann (1972) for "anarakite" remained unexplained, but type "anarakite" contains more Zn than was found in the material examined here. Thus, we speculated that the role of Zn is possibly structurally crucial, and this aspect was accordingly examined in a series of synthesis experiments.

SYNTHESIS PROCEDURES AND ANALYTICAL METHODS

All syntheses were conducted using reagent-grade chemicals and the direct precipitation procedure outlined by Sharkey & Lewin (1971). A known volume of solution containing appropriate concentrations of CuCl_2 , ZnCl_2 , or $\text{Zn}(\text{NO}_3)_2$ was placed in a glass reactor, which was heated to 95°C to minimize the possible formation of amorphous phases. A known volume of NaOH solution at room temperature was pumped at a constant rate (≤ 100 mL/h) into the hot

reactor to initiate the precipitation reaction. When all the NaOH solution had been added, the resulting hot slurry was filtered; the precipitate was washed with water and was dried at 110°C prior to chemical analysis and mineralogical study. Test variables for the syntheses included the concentrations of the various metal ions, the solution pH, the ratio of NaOH/M^{2+} , the method and rate of reagent addition, and the effect of nitrate *versus* chloride anions.

For chemical analysis, the dried samples were dissolved in 1:1 HNO_3 and were diluted to an appropriate volume. Concentrations of Cu, Zn, Ni, and Co were determined by atomic absorption spectroscopy with matrix-matched standards. Chlorine was determined by high-pressure liquid chromatography and by ion-selective electrodes, with the two methods yielding comparable results.

X-ray-diffraction data for the synthetic Cu–Zn products were collected mainly with a Rigaku rotating-anode diffractometer operated at 55 kV, 180 mA, using a curved-crystal graphite monochromator and $\text{CuK}\alpha$ radiation. Indexing and unit-cell refinement utilized the program POWLS, a routine originally written by E.J. Gabe and subsequently modified by J.T. Szymański. As only small quantities of material were available for some samples, all were mounted with acetone on a "zero-background" plate scanned at 4° 2 θ per minute, and all peak maxima were checked manually. An iterative procedure was employed in the least-squares refinements, with several cycles used in the progression from low-angle intense lines to the higher-angle lines. Special attention was paid to peak widths, and any lines showing broadening attributable to overlap of lines were disregarded in the final refinements.

Effect of CuCl_2 concentration

To define the preferred concentration of CuCl_2 for the synthesis, 200 mL of NaOH solution were pumped at 100 mL/h into 200 mL of CuCl_2 solution heated to 95°C. The CuCl_2 solution initially was at its natural pH value of approximately 2, and the CuCl_2 concentration was varied from 0.15 to 1.0 M; the molar ratio $\text{OH}^-/\text{Cu}^{2+}$ was fixed at unity in all the experiments. The products made from solutions containing 0.5 or 1.0 M CuCl_2 were difficult to filter and contained grains of a dark phase; the products were subsequently shown by X-ray-diffraction analysis to contain CuO in addition to the monoclinic phase of $\text{Cu}_2(\text{OH})_3\text{Cl}$ as synthesized by Oswald & Guenter (1971). By contrast, the products synthesized from the more dilute CuCl_2 solutions consisted only of the monoclinic phase, containing approximately 60% Cu and 16% Cl [ideal $\text{Cu}_2(\text{OH})_3\text{Cl}$: 64.19% Cu, 16.60% Cl, 23.89 wt.% OH]. A slight excess of water was recorded in all of the analyses even though the precipitates were dried for 24 h at 110°C. A relatively constant 2.6–2.7 g of precipitate were formed for CuCl_2 concentrations ranging from 0.15 to 0.25 M.

Similar results were obtained when 0.15–0.25 M CuCl_2 solutions were pumped into an equal concentration of NaOH solution heated to 95°C. On the basis of these results, most of the subsequent experiments were done by pumping NaOH solution into a 0.2 M CuCl_2 solution heated to 95°C.

Effect of ZnCl_2 and $\text{Zn}(\text{NO}_3)_2$ concentrations

Figure 1 illustrates the effect of the Zn chloride concentration on the compositions of the products made by pumping 300 mL of 0.066 M NaOH at 100 mL/h into 100 mL of 0.2 M CuCl_2 solution at 95°C; i.e., 0.02 moles of NaOH were added to 0.02 moles of CuCl_2 . In all instances, a relatively constant 1.2–1.5 g of precipitate were formed. Chemical analysis of the precipitates showed that the Zn content increased systematically as the ZnCl_2 concentration of the 0.2 M CuCl_2 solution was increased from 0.0 to 5.5 M ZnCl_2 . The Cu content of the precipitates decreased as the Zn content increased. X-ray-diffraction analysis of the products indicated only $\text{Cu}_2(\text{OH})_3\text{Cl}$ or $(\text{Cu,Zn})_2(\text{OH})_3\text{Cl}$.

Similar results were obtained when using a stoichiometric deficiency of NaOH in a CuCl_2 solution containing added ZnCl_2 ; Figure 2 illustrates the compositions of the products made in experiments where 100 mL of 0.1 M NaOH were pumped at 6 mL/h into 200 mL of 0.2 M CuCl_2 solutions containing various concentrations of ZnCl_2 . In these tests, only 0.01 moles of NaOH were added to 0.04 moles of

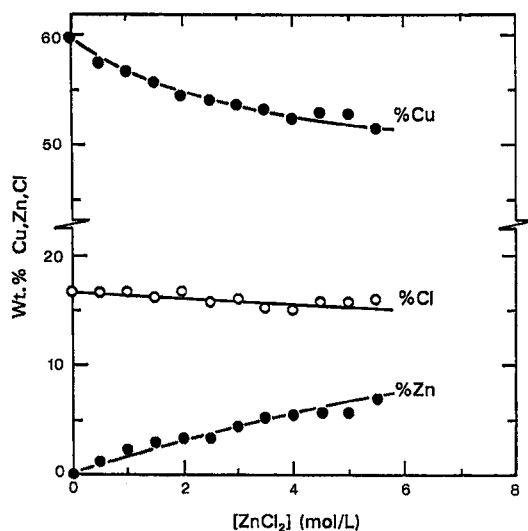


FIG. 1. Effect of ZnCl_2 concentrations on the compositions of the products made by pumping 300 mL of 0.066 M NaOH, at 100 mL/h, into 100 mL of 0.2 M CuCl_2 solution at 95°C.

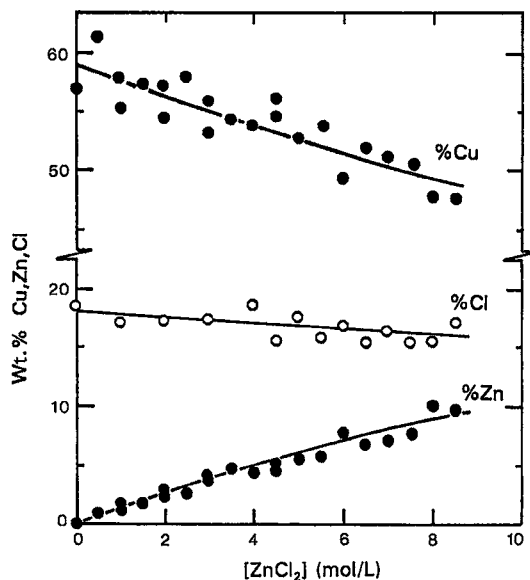


FIG. 2. Compositions of the products obtained by addition of 0.1 M NaOH to 0.2 M CuCl_2 solutions containing various concentrations of ZnCl_2 .

CuCl_2 , and the resulting product weights were typically 0.3 to 1.3 g. As the ZnCl_2 concentration of the CuCl_2 solution increased from 0 to 8.5 M ZnCl_2 , the Zn content of the precipitate increased from 0 to about 9% Zn. The trend is comparable to that shown in Figure 1, and as the Zn content increases, the Cu content declines. The Cl content drops slightly with increasing ZnCl_2 concentration, and this observation also is consistent with the data illustrated in Figure 1. All the products were shown by X-ray-diffraction analysis to consist only of $\text{X}_2(\text{OH})_3\text{Cl}$ -type compounds ($\text{X} = \text{Cu}$ or Cu,Zn).

Figure 3 illustrates the corresponding results obtained when 300 mL of 0.066 M NaOH solution (0.02 moles) were pumped at 100 mL/h into 100 mL of 0.2 M CuCl_2 solution (0.02 moles) containing various concentrations of $\text{Zn}(\text{NO}_3)_2$. The results are approximately the same as those obtained in the presence of ZnCl_2 . Increasing the Zn concentrations of the CuCl_2 solution resulted in an increase in the Zn content of the product, and a corresponding decrease in the Cu content. The Cl content also declined slightly. The presence of 4 M $\text{Zn}(\text{NO}_3)_2$ resulted in a product containing approximately 9% Zn, whereas a 4 M ZnCl_2 solution gave a precipitate containing about 5% Zn. X-ray-diffraction analysis showed the products made from solutions containing 0 to 4 M $\text{Zn}(\text{NO}_3)_2$ to consist only of $\text{X}_2(\text{OH})_3\text{Cl}$ -type compounds; by contrast, $\text{Zn}(\text{NO}_3)_2$ concentrations greater than 4 M resulted in the precipitation of zincian gerhardtite, $(\text{Cu,Zn})(\text{NO}_3)(\text{OH})$.

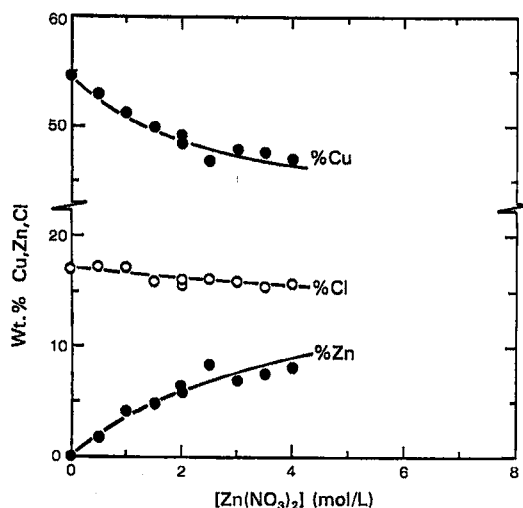


FIG. 3. Compositions of the products obtained by addition of 0.066 M NaOH to 0.2 M CuCl_2 solutions containing various concentrations of $\text{Zn}(\text{NO}_3)_2$.

Attempts to prepare the end-member Zn analogue of $\text{Cu}_2(\text{OH})_3\text{Cl}$ by pumping NaOH into various ZnCl_2 - $\text{Zn}(\text{NO}_3)_2$ solutions at 95°C were unsuccessful. The pumping of small amounts of NaOH did not cause any Zn precipitation, whereas the addition of large amounts of NaOH resulted in the precipitation of simonkolleite, $\text{Zn}_5(\text{OH})_8\text{Cl}_2 \cdot \text{H}_2\text{O}$.

Effect of $(\text{OH})^-/\text{Cu}^{2+}$ molar ratio

To investigate the effect of the $(\text{OH})^-/\text{Cu}^{2+}$ molar

ratio on the amount and composition of the products, 200 mL of solution containing 0.2, 0.15, 0.10, or 0.07 M NaOH were pumped at 6 mL/h into 200 mL of 0.2 M CuCl_2 - 4 M ZnCl_2 solution at 95°C. The NaOH/ CuCl_2 molar ratio seems to have had little effect on the composition of the precipitates, which consistently contained about 52% Cu, 5% Zn, and 15% Cl. The principal effect of decreasing the relative amount of NaOH was that the amount of precipitate decreased linearly with the concentration of NaOH.

X-RAY STUDY OF SYNTHETIC PRODUCTS

The products of the syntheses are fine-grained green to greenish blue powders, the latter reliably indicating a substantial uptake of Zn. All of the products were examined visually by Guinier - de Wolff X-ray patterns obtained with Co X-radiation. The patterns were classified into two groups, one being that of the simpler pattern characteristic of our specimens of the Anarak mineral, and the other referring to the slightly more complex pattern typical of the monoclinic $\text{Cu}_2(\text{OH})_3\text{Cl}$ phase synthesized by Oswald & Guenter (1971; PDF 25-1427). Preliminary unit-cell dimensions, based on a hexagonal cell with a 6.84, c 14.06 Å, were subsequently determined by least-squares refinements of partial diffractometry data. Plots of a and c versus Zn in atoms per formula unit showed that the transition from the Oswald & Guenter (1971) monoclinic phase to the Cu-Zn rhombohedral phase occurs approximately between $\text{Cu}_{94}\text{Zn}_6$ and $\text{Cu}_{91}\text{Zn}_9$ (Fig. 4). The transition zone in some patterns was found to be clearly recognizable by a merging of diffraction lines, but there was some overlap in the classification of individual samples within the zone (Fig. 4).

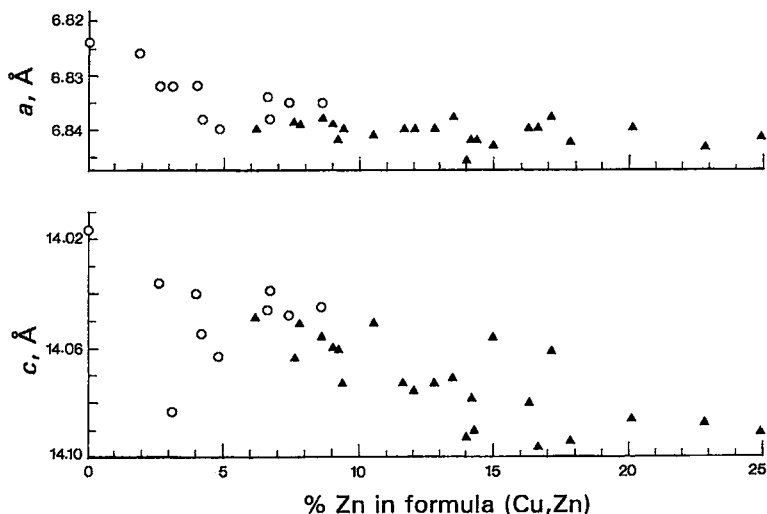


FIG. 4. Plot of a and c dimensions versus formula percentage Zn in synthetic $(\text{Cu,Zn})_2(\text{OH})_3\text{Cl}$ (Table 3). Open circles: monoclinic phase; solid triangles: hexagonal phase. All samples indexed on a hexagonal cell.

TABLE 3. SYNTHETIC $(\text{Cu}_x\text{Zn}_{1-x})(\text{OH})_3\text{Cl}$ SERIES INDEXED WITH HEXAGONAL CELL

Sample number	Formula % Zn	<i>a</i> (Å)	<i>c</i> (Å)	Type
1-6	0	6.824(13)	14.017(21)	M
AD-2	1.9	6.826(7)	14.107(19)	M
44	2.6	6.832(6)	14.036(8)	M
7	3.1	6.832(3)	14.083(8)	M
45	4.0	6.832(11)	14.040(11)	M
AD-3	4.2	6.838(8)	14.055(16)	M
AD-4	4.8	6.840(7)	14.063(15)	M
P104	6.2	6.840(1)	14.049(3)	H
PARA 46	6.6	6.834(5)	14.046(7)	M
P19	6.7	6.838(4)	14.039(5)	M
P8	7.4	6.835(8)	14.048(14)	M
P51A	7.6	6.839(1)	14.064(2)	H
P20	7.8	6.839(1)	14.051(3)	M
P9	8.6	6.835(3)	14.045(6)	M
P23	8.6	6.838(1)	14.056(1)	H
P24	9.0	6.839(1)	14.060(1)	H
P48	9.2	6.842(2)	14.061(4)	H
P51B	9.4	6.840(1)	14.073(2)	H
P10	10.5	6.841(1)	14.051(2)	H
P51C	11.6	6.840(1)	14.073(2)	H
P50	12.0	6.840(2)	14.076(2)	H
P51D	12.8	6.840(1)	14.073(2)	H
P49	13.5	6.838(3)	14.071(6)	H
P47	14.0	6.846(7)	14.093(9)	H
P15	14.2	6.842(1)	14.079(2)	H
P38	14.3	6.842(4)	14.090(7)	H
P12	15.0	6.843(1)	14.056(3)	H
P39	16.3	6.840(1)	14.080(3)	H
P51E	16.6	6.840(3)	14.096(4)	H
P51F	17.1	6.838(1)	14.062(2)	H
P41	17.8	6.845(2)	14.094(3)	H
P42	20.1	6.840(1)	14.086(3)	H
P36	22.8	6.844(4)	14.088(5)	H
P37	24.9	6.842(5)	14.091(10)	H

M = monoclinic, H = hexagonal

in most samples, several diffraction lines in the patterns are extraneous to the rhombohedral cell of paratacamite as given by Frondel (1950). These extraneous lines were satisfactorily indexable with the monoclinic cell of Oswald & Guenter (1971).

Thus, the initial premise that the synthesis series would indicate a transition from a Cu end-member represented by paratacamite (rhombohedral) to a potentially monoclinic Zn-rich member was exactly the reverse of what was found, *i.e.*, the synthetic Cu end-member is monoclinic, and the Zn-rich members are rhombohedral. The maximum Zn content of the synthetic series is 14.8 wt.%, corresponding to $(\text{Cu}_{1.50}\text{Zn}_{0.50})(\text{OH})_3\text{Cl}$, which is higher than the Zn content of "anarakite" as described by Adib & Ottemann (1972). The poorer quality, as marked by increased diffuseness of the X-ray patterns, of the two most Zn-rich samples in the series (Fig. 4) suggests that the upper limit of Zn substitution in our synthetic paratacamite (rhombohedral) may have been closely approached. However, Kracher & Pertlik (1983) obtained an electron-microprobe analysis of paratacamite from the Herminia mine, Chile, in which the Zn content is 16.2 wt.%; this zincian paratacamite was confirmed by them to be rhombohedral, space group $R\bar{3}$, with cell dimensions as reported by Fleet (1975). The monoclinic synthetic phase seems to be less tolerant of Zn incorporation, and the upper limit was found to be about 9 wt.% Zn. In monoclinic samples with Zn contents in this range (P8, P9, P20; Table 3), doublet diffraction lines are close to merging, leading to a more simple pattern that approaches that of the rhombohedral phase.

THE NEW MINERAL CLINOATACAMITE

The preliminary X-ray results showed that there are problems in indexing all of the diffraction lines on the basis of a hexagonal cell. Subsequent collection of precise diffractometry data confirmed that, although a small amount of contamination by atacamite is present

This study of paratacamite was initiated because differences were observed in the X-ray patterns of natural specimens of paratacamite. When it became apparent from the synthesis experiments that neither

TABLE 4. UNIT CELLS OF CLINOATACAMITE AND RELATED Cu, (Cu,Zn), AND Co PHASES

	$\text{Cu}_2(\text{OH})_2\text{Cl}$ botallackite (PDF 8-88)	$\text{Cu}_2(\text{OH})_2\text{Cl}$ anacamite (PDF 23-948)	$(\text{Cu}_x\text{Zn}_{1-x})(\text{OH})_3\text{Cl}$ "anarakite" (PDF 25-325)	$(\text{Cu}_x\text{Zn}_{1-x})(\text{OH})_3\text{Cl}$ paratacamite (Chite) ²	$\text{Cu}_2(\text{OH})_2\text{Cl}$ synthetic (PDF 25-1427) ³	$\text{Cu}_2(\text{OH})_2\text{Cl}$ clinoatacamite (synthetic) ⁴	$\text{Cu}_2(\text{OH})_2\text{Cl}$ clinoatacamite (this study) ⁵	$\text{Co}_2(\text{OH})_2\text{Cl}$ (synthetic) ⁶
<i>a</i> , Å	5.715	6.892	11.901	13.654	11.83	6.17	6.157	6.84
<i>b</i> , Å	6.124	9.080	6.830	—	6.822	6.82	6.814	—
<i>c</i> , Å	5.632	6.055	10.162	14.041	6.166	9.12	9.105	14.50
β°	92.75	—	112.87	—	130.62	99.63	99.65	—
system*	M	O	M	R	M	M	M	R
space group	$P2_1/m$	$Pm\bar{c}n$	$Cc, C2/c$	$R\bar{3}$	$P2_1/a$	$P2_1/n$	$P2_1/n$	$R\bar{3}m$

*M = monoclinic, O = orthorhombic, R = rhombohedral

1. Adib & Ottemann (1972), Kati Kati mine, Anarak, Iran

2. Fleet (1975), Sierra Gorda, Chile; same cell from single-crystal X-ray methods by Frondel (1950) and Pring *et al.* (1987)

3. Oswald & Guenter (1971), synthetic "paratacamite" (= clinoatacamite)

4. Reduction (this study) of the Oswald & Guenter (1971) cell; note the dimensional similarity, with axes interchanged, to the parameters of atacamite

5. Chunguicamata, Chile (M32176)

6. de Wolff (1953)

the "anarakite" cell nor Zn substitution could explain the observed differences, which were thought to exist at end-member compositions in natural material, it was concluded that natural "paratacamite" exists in two structurally distinct forms. One of these corresponds to the classical rhombohedral form (Palache *et al.* 1951), which was structurally described by Fleet (1975), and the other corresponds to the monoclinic phase synthesized by Oswald & Guenter (1971) and Walter-Levy & Goreaud (1969; PDF 23-947, indexed with hexagonal axes). Without wishing to be repetitive, we reiterate that the monoclinic unit cell of this synthetic phase differs from that of botallackite, but can be indirectly related to the monoclinic unit cell that was derived by Adib & Ottemann (1972) for "anarakite" (Table 4). The proposal that the new monoclinic phase be called *clinoatacamite* has been approved by the Commission on New Minerals and Mineral Names, International Mineralogical Association. The new name alludes to the difference in symmetry from atacamite and paratacamite. Clinoatacamite has been found in specimens from several localities; the specimen designated as the holotype is from Chuquicamata, Chile, and is part of the collection of the Royal Ontario Museum (M32176).

Crystallography

Single-crystal X-ray study of clinoatacamite was done on a fragment from a specimen labeled as paratacamite, bench C-2, north end, open-pit mine, Chuquicamata, Chile (M32176). Clinoatacamite is monoclinic, space group $P2_1/n$, a 6.157(2), b 6.814(3), c 9.104(5) Å, β 99.65(4)° as refined from the X-ray powder pattern given in Table 1. No superstructure was observed, and the structure was resolved to residual indices $R = 5.2$ and $R_w = 4.9\%$. Details of the structure are presented in a companion paper (Grice *et al.* 1996). All Cu-octahedra in clinoatacamite display Jahn-Teller distortion.

The synthetic phase prepared by Oswald & Guenter (1971) was described by them as monoclinic, space group $P2_1/a$, a 11.83(1), b 6.822(3), c 6.166(5) Å, β 130.62(3)°. This cell can be reduced to a 6.166, b 6.822, c 9.11 Å, β 99.71°, space group $P2_1/n$; in comparison, the cell derived from the single-crystal structure study of clinoatacamite gave a 6.144, b 6.805, c 9.112 Å, β 99.55°. Transformation of the latter cell to show the relationship to paratacamite gives a pseudo-hexagonal cell with a 13.610, b 13.626, c 14.031 Å, α 89.47°, β 90.00°, γ 119.96°; thus, a is equal to 13.6 and c is equal to 14.03 Å, and both are similar to those of paratacamite (Table 4).

Physical and optical properties

Clinoatacamite has been found on specimens from several localities. The mineral varies from green to

dark greenish black, less commonly greenish blue. The morphology varies from simple, twinned pseudorhombic grains up to 1 mm across, to complicated intergrowths of euhedra, exactly as for paratacamite and megascopically indistinguishable from it. The luster is adamantine, but fine-grained powdery aggregates with a vitreous luster also occur. The mineral is transparent to translucent, brittle, nonfluorescent, $H = 3$, and has an even fracture. A perfect cleavage is present; the cleavage face was checked by a precession X-ray photograph and was determined to be {012}. Crystals are generally twinned on (100). The calculated density using the ideal formula $\text{Cu}_2(\text{OH})_3\text{Cl}$ and $Z = 4$ is 3.77 g/cm³, which is similar to that of paratacamite. The measured density could not be determined because its value is too high for standard heavy liquids, and because of the lack of abundant material. This shortage is related to the uncertain megascopic distinction from paratacamite, and the recognition that the two minerals coexist on individual specimens. The morphological similarity is highlighted by the knowledge that clinoatacamite coexists with paratacamite in the holotype specimen of paratacamite from Sierra Gorda, Chile (The Natural History Museum, specimen BM 86958); this specimen was one of several used by Frondel (1950) in his description of paratacamite, and was the source of the crystal used by Fleet (1975) for the structure determination of paratacamite. Thus, it was deemed necessary to deal with these minerals on a grain-by-grain basis rather than resorting to bulk samples.

Clinoatacamite has high indices of refraction, but these could not be determined because of reaction with the immersion liquids. The mineral is biaxial negative, $2V_{\text{meas}} = 75(5)^\circ$, $2V_{\text{calc}} = 69(3)^\circ$ by extinction curves. Dispersion is strong, $r \ll v$; orientation is $X = b$, $Y:a = 10^\circ$, in obtuse angle β . No pleochroism was observed. The optical properties of clinoatacamite thus are distinct from those of paratacamite. Paratacamite, however, has also been reported to be biaxial, with $2V$ up to about 50° and $r > v$ (Fron del 1950, Palache *et al.* 1951). Adib & Ottemann (1972) reported "anarakite" to be biaxial positive, $2V = 40^\circ$, n_α 1.842, n_γ 1.849, pleochroic from green to grass green. Our optical examination of zincian paratacamite from Anarak shows that the crystal aggregates consist of hexagonal plates about 10 μm across, $n > 1.800$, nonpleochroic, uniaxial negative, but with some grains giving biaxial figures with a $2V$ of about 5° .

The optical properties reported by Adib & Ottemann (1972) for "anarakite" are similar to those reported by Frondel (1950) for "biaxial paratacamite" from the Sierra Gorda mine, Chile (BM 86958). As our examination of the same specimen (BM 86958) revealed that it contains both zincian paratacamite and clinoatacamite, we infer that the "biaxial paratacamite" observed by Frondel (1950) is clinoatacamite. This inference is further supported by our re-examination of

a cotype specimen of "paratacamite" from Remolinos, Chile (USNM 95146), which also was used in the description of paratacamite by Frondel (1950). Energy-dispersion analyses of thirteen grains confirmed them to be Zn-free, as reported in Frondel (1950), but X-ray-diffraction patterns of four grains showed all to be clinoatacamite rather than paratacamite. Nevertheless, various discrepancies in the optical properties remain unexplained; most notable is that we find paratacamite to be uniaxial negative, whereas the sign is reported as uniaxial positive in Palache *et al.* (1951).

Composition

Electron-microprobe analyses of grains from the Chuquicamata specimen (M32176) were obtained using a JEOL 733 instrument operated at 13 kV, with a ZAF correction program and CuS (Cu) and NaCl (Cl) as standards. Zinc and Ni were not detected. The mean analytical results (and ranges) are: CuO 74.7 (73.4–76.0), Cl 16.5 (15.7–17.2), $(\text{H}_2\text{O})_{\text{calc}}$ 13.5, sum 104.7, less O \equiv Cl 3.7, total 101.0 wt.%. The empirical formula for O + Cl = 4 is $\text{Cu}_{1.96}\text{O}_{3.03}\text{H}_{3.11}\text{Cl}_{0.97}$, ideally $\text{Cu}_2(\text{OH})_3\text{Cl}$. The latter requires CuO 74.49, Cl 16.60, H_2O 12.66, sum 103.75, less O \equiv Cl 3.75, total 100 wt.%.

Distribution

Clinoatacamite from Chuquicamata, Chile (M32176), occurs with atacamite, paratacamite, gypsum, and alunite on a quartzose matrix. Clinoatacamite also was found in a specimen from Calumet, Michigan (ROM, M26081), from Mason Pass, Lyon County, Nevada (Cureton 4731), from Chuquicamata, Chile (Pinch 508), from Sierra Gorda mine, Chile (BM 86958), from Wallaces Gully, Mount Painter, South Australia (South Australian Museum G13208), from Wallaroo mines, Kadina, South Australia (South Australian Museum G11409), and from Remolinos, Chile (USNM 95146). Three specimens from the type locality for "anarakite" (Kali Kafi mine, Anarak Province, Iran), but obtained from three different sources (ROM M35449; National Mineral Collection NMC 14654; Pinch collection "zincrosasite") proved to be paratacamite. Additional specimens that proved to be paratacamite are from Churchill Buttes, Lyon County, Nevada (M23078), from Levant mine, Cornwall, England (M32265), from Nangeroo mine, Murrin Murrin, Western Australia (M33193), from the Carr Boyd nickel mine, Western Australia (unnumbered, Cureton), and from the Otter Shoot, Kambalda, Western Australia (South Australian Museum G12245). The Carr Boyd and Otter Shoot specimens gave slightly different X-ray patterns, and proved to be nickeliferous.

The above study shows that atacamite commonly coexists with paratacamite and clinoatacamite. In some

specimens, such as those from Sierra Gorda and the holotype from Chuquicamata, all three minerals coexist.

The relative stabilities of atacamite and paratacamite have been widely discussed, most recently by Woods & Garrels (1986), Pollard *et al.* (1989), Butuzova *et al.* (1989), and Hannington (1993). Pollard *et al.* (1989) concluded that paratacamite is the thermodynamically stable phase at ambient temperatures. It is possible, however, that the phase synthesized by Pollard *et al.* was clinoatacamite rather than paratacamite, exactly as was the case in the experiments by Walter-Levy & Goreaud (1969), Oswald & Guenter (1971), Sharkey & Lewin (1971), and in this study. There is general agreement that botallackite, which is of limited natural occurrence, is metastable with respect to the other $\text{Cu}_2(\text{OH})_3\text{Cl}$ polymorphs. Of these, atacamite is probably the most widespread in geological occurrence.

SUBSTITUTIONS OF Co AND Ni FOR Cu

In the experimental studies concerning Zn substitution, it was shown that partial solid-solution occurs in clinoatacamite, and more extensively in paratacamite. The supercell reflections in zincian paratacamite are extremely weak, and unless special precautions are taken to detect the full cell, the apparent cell corresponds to a 6.8, c 14.0 Å, possible space-group $R\bar{3}m$. Rhombohedral compounds with these cell dimensions and space group $R\bar{3}m$ are known as the synthetic phases $\text{Fe}_2(\text{OH})_3\text{Cl}$, $\text{Mn}_2(\text{OH})_3\text{Cl}$, and $\text{Co}_2(\text{OH})_3\text{Cl}$. In his description of the structure of $\text{Co}_2(\text{OH})_3\text{Cl}$, de Wolff (1953) suggested that $\text{Cu}_2(\text{OH})_3\text{Cl}$ might also be included in this structural type. This possibility was accordingly examined in a series of synthesis experiments.

Co–Cu synthesis experiments

$\text{Co}_2(\text{OH})_3\text{Cl}$ was synthesized by pumping 200 mL of 0.2 M NaOH solution at 25 mL/h into 200 mL of 0.2 M CoCl_2 medium held at 95°C. The X-ray pattern of the precipitate is distinct from that of paratacamite, and is in good agreement with the powder data given by de Wolff (1953) for $\text{Co}_2(\text{OH})_3\text{Cl}$.

The effect of the concentration of CoCl_2 on the synthesis of $\text{Cu}_2(\text{OH})_3\text{Cl}$ was investigated by adjusting the 0.2 M CuCl_2 medium to 0.2 M ($\text{CoCl}_2 + \text{CuCl}_2$). That is, the Cu concentration of the solution decreased as the Co concentration increased. Increasing the CoCl_2 concentration from 0.0 to 0.05 M had little effect on the composition of the products; the Cu content was approximately 57%, and the Co content was consistently less than 1 wt.%. Increasing the CoCl_2 concentration to greater than 0.05 M, with concomitant reductions in the CuCl_2 concentrations, caused a linear increase in the Co content of the products and a

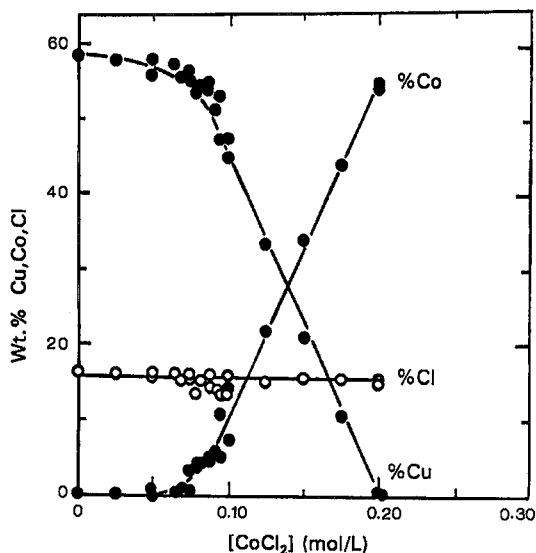


FIG. 5. Compositions of the products obtained by addition of 0.2 M NaOH to 0.2 M ($\text{CuCl}_2 + \text{CoCl}_2$).

simultaneous linear decrease in the Cu content (Fig. 5). In all the syntheses, the Cl content remained relatively constant at about 15% Cl.

Guinier - de Wolff X-ray diffraction patterns of the precipitates showed that cobaltoan clinatoacamite was formed to a maximum of 5 wt.% Co, *i.e.*, $(\text{Cu}_{1.83}\text{Co}_{0.17})(\text{OH})_3\text{Cl}$. Bulk samples containing higher Co values were found to be two-phase mixtures of clinatoacamite and rhombohedral $\text{Co}_2(\text{OH})_3\text{Cl}$. As for the Cu-Zn series, however, the transformation boundary is not sharp: two-phase products were found in samples containing as little as 3.2 wt.% Co. Thus, the rhombohedral Co phase is distinct, and relatively little Co substitution was effected with the conditions of synthesis that were utilized.

Ni-Cu synthesis experiments

Efforts to prepare $\text{Ni}_2(\text{OH})_3\text{Cl}$ or Ni-bearing $\text{Cu}_2(\text{OH})_3\text{Cl}$ were not overly successful, as is indicated by the data in Figure 6. The experimental conditions were similar to those conducted for Co. Increasing the NiCl_2 concentration from 0.0 to 0.05 M had little effect on the composition of the product; the Cu, Cl, and Ni contents are approximately 61%, 15%, and less than 0.5 wt.%, respectively. X-ray-diffraction patterns showed these products to contain single-phase clinatoacamite. Increasing the concentration of NiCl_2 beyond 0.05 M resulted in a rapid increase in the Ni content of the products and a corresponding decline in the Cu content; significantly, however, the Cl content

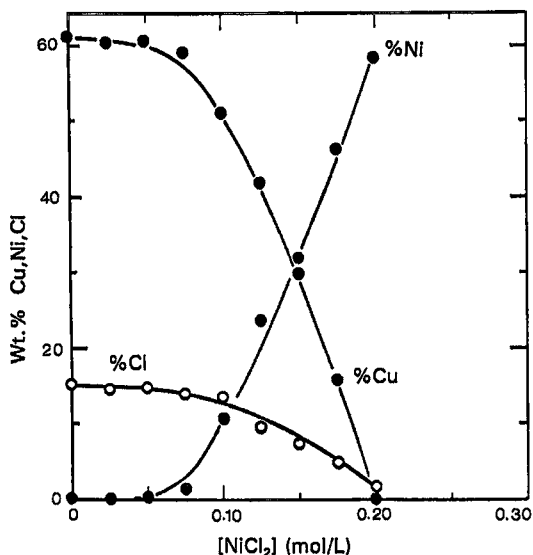


FIG. 6. Compositions of products obtained by addition of 0.2 M NaOH to 0.2 M ($\text{CuCl}_2 + \text{NiCl}_2$).

also decreased systematically. X-ray-diffraction analysis of the products made from solutions containing more than 0.05 M NiCl_2 showed increasing amounts of $\text{Ni}(\text{OH})_2$. The X-ray results, coupled with the reduced Cl contents, indicated that the increase in the Ni content of the precipitates was due to the admixture of $\text{Ni}(\text{OH})_2$ and $\text{Cu}_2(\text{OH})_3\text{Cl}$.

Efforts to suppress the formation of $\text{Ni}(\text{OH})_2$ by varying the amount of NaOH pumped (0.1 or 0.2 M NaOH), by decreasing the pH of the NiCl_2 - CuCl_2 solution from 5.5 to 2.5, or by increasing the total chloride content of the NiCl_2 - CuCl_2 solution by the addition of 0.2 to 2.0 M LiCl, were unsuccessful. Nickel hydroxide was detected in major amounts in all products. Although a Co analogue of $\text{Cu}_2(\text{OH})_3\text{Cl}$ exists, we were not able to synthesize the corresponding Ni analogue.

Nickeliferous paratacamite

Although we were unable to effect an uptake of Ni by $\text{Cu}_2(\text{OH})_3\text{Cl}$, the paratacamite from the Carr Boyd nickel mine, Western Australia, shows X-ray diffraction-line shifts that are caused by the presence of appreciable amounts of Ni in solid solution. Electron-microprobe analysis showed some variation in Ni-Cu ratios, and seven quantitative analyses gave an average (and range) of Cu 49.9 (48.1-52.7), Ni 8.5 (6.4-10.3), Cl 16.0 (14.1-16.7), $(\text{OH})_{\text{calc}}$ 25.6 (25.0-26.8). The composition with the highest Ni content (10.3 wt.%) corresponds to $(\text{Cu}_{1.62}\text{Ni}_{0.38})(\text{OH})_{3.15}\text{Cl}_{1.00}$, and the

TABLE 5. X-RAY POWDER DATA FOR NICKELIFEROUS PARATACAMITE, CARR BOYD MINE, WESTERN AUSTRALIA

l_{est}	d_{meas}	d_{calc}	hkl	l_{est}	d_{meas}	d_{calc}	hkl
100	5.44	5.449	101	<5	1.743	1.744	125
25	4.62	4.637	003	40	1.710	1.710	220
10	4.51	4.509	012	<5	1.666	1.660	222
15	3.415	3.420	110	<5	1.650	1.650	027
5	3.004	2.999	104	5	1.630	1.631	131
45	2.899	2.897	021	5	1.602	1.604	223
80	2.751	2.752	113	10	1.500	1.500	208
25	2.725	2.725	202	15	1.485	1.486	217
15	2.316	2.319	006	5	1.472	1.472	401
70	2.253	2.255	024	10	1.448	1.448	042
<5	2.212	2.210	211	5	1.409	1.409	119
15	2.026	2.028	205	20	1.376	1.376	226
<5	1.918	1.919	116	10	1.363	1.362	404
15	1.884	1.884	107	5	1.353	1.352	321
30	1.816	1.817	033	<5	1.308	1.307	045

114.54-mm Gandolfi film, CoK α radiation. Indexed with hexagonal subcell a 6.839(2), c 13.911(4) Å.

average composition is $(\text{Cu}_{1.69}\text{Ni}_{0.31})(\text{OH})_{3.24}\text{Cl}_{0.97}$. The cell dimensions from the indexed powder pattern (Table 5) are similar to those of zincian paratacamite.

Optical examination of the Carr Boyd nickeliferous paratacamite showed it to be uniaxial negative. Nickel *et al.* (1994) reported the occurrence of nickeloan paratacamite with up to 17.4 wt.% Ni at the Widgiemooltha deposit, Western Australia, and it too is uniaxial negative (E.H. Nickel, written comm., 1994).

CONCLUSIONS

Clinoatacamite is the third well-defined polymorph of $\text{Cu}_2(\text{OH})_3\text{Cl}$, and will be the fourth if it is demonstrated that paratacamite exists at the end-member composition. Although the original analysis of paratacamite from the Generosa mine, Chile (BM 86958) did not report the presence of Zn (Smith 1906), subsequent electron-microprobe analysis by Embrey & Jones (in Kracher & Pertlik 1983) showed that this specimen contains 2.45 wt.% Zn, which we have confirmed for our portion of the specimen. Thus the fragment used by Fleet (1975), also from the same specimen, for the X-ray structure study of paratacamite is likely Zn-bearing, as had been deduced by Kracher & Pertlik (1983), Effenberger (1989), and Burns (1994). Kracher & Pertlik (1983) suggested that the structure of paratacamite is stabilized, relative to those of atacamite and botallackite, by the partial substitution of Zn for Cu in paratacamite. The results obtained here support the concept that the formation of paratacamite is favored by the presence of substituting cations such as Zn or Ni, even though these may be as little as 2–3 wt.%. In the absence of these cations, the mineral more likely to form is clinoatacamite rather than paratacamite.

The results of this study add to the doubts about

the validity of "anarakite". The observation in the synthesis experiments that high Zn contents in $(\text{Cu,Zn})_2(\text{OH})_3\text{Cl}$ lead to the formation of paratacamite (rhombohedral) rather than a monoclinic structure is at variance with the monoclinic symmetry reported for "anarakite". The specimens examined here from the type locality for "anarakite" indicate that there is substantial variation in the ratio of Cu:Zn, and possibly the fragment examined by Adib & Ottemann (1972) by single-crystal X-ray methods differed in composition from their chemically analyzed sample. The recognition by Kracher & Pertlik (1983) that the unit cell of "anarakite" can be transformed to that of the monoclinic synthetic phase of Oswald & Guenter (1971) is significant in that this synthetic phase corresponds to the mineral now called clinoatacamite. Thus, it is possible to speculate that the single-crystal fragment of "anarakite" may have been clinoatacamite.

The X-ray powder patterns of atacamite and botallackite are distinct from each other and from those of paratacamite and clinoatacamite. The pattern of clinoatacamite is slightly more complex than that of paratacamite, and one of the distinguishing features is the clustering of four diffraction lines at 2.713, 2.339, 2.266, and 2.243 Å for clinoatacamite, whereas only two lines appear in this range for paratacamite (Table 1). Published X-ray patterns for synthetic "paratacamite", including the PDF standard for paratacamite (25–1427), pertain to clinoatacamite rather than paratacamite.

ACKNOWLEDGEMENTS

The assistance of CANMET personnel D.R. Owens and T.T. Chen (microbeam laboratory), P. Carrière (X-ray), and O. Dinardo (syntheses) is much appreciated. Specimens of paratacamite and related minerals examined in this study were kindly provided by J.A. Mandarino and R.I. Gait (Royal Ontario Museum), A.J. Criddle (The Natural History Museum), H.G. Ansell (National Mineral Collection, Geological Survey of Canada), W.W. Pinch (Rochester, N.Y.), A. Pring (South Australian Museum), and P.J. Dunn (Smithsonian Institution). Editorial comments by R.F. Martin and critical reviews by C.N. Alpers and P.C. Burns were of significant benefit, and we are particularly grateful to Dr. Burns for bringing to our attention the publication by Kracher & Pertlik (1983).

REFERENCES

- ADIB, D. & OTTEMANN, J. (1972): Ein neues mineral, $(\text{Cu,Zn})_2(\text{OH})_3\text{Cl}$, aus der Kali-Kafi mine, Provinz Anarak, zentral Iran. *Neues Jahrb. Mineral., Monatsh.*, 335–338.
- BURNS, P.C. (1994): *The Stereochemistry of Cu^{2+} Oxysalt Minerals: an Ab Initio Molecular Orbital Approach*. Ph.D. thesis, Univ. Manitoba, Winnipeg, Manitoba.

- BUTUZOVA, G.YU., SHTERENBERG, L.YE., VORONIN, B.I. & GOR'KOVA, N.V. (1989): Atacamite in metalliferous sediments of the Atlantic. *Dokl. Earth Sci.* **309**, 158-161.
- EFFENBERGER, H. (1989): An uncommon $\text{Cu}^{2+4}\text{O}_6$ coordination polyhedron in the crystal structure of $\text{KCu}_3(\text{OH})_2[(\text{AsO}_4)_2\text{H}(\text{AsO}_4)]$ (with a comparison to related structure types). *Z. Kristallogr.* **188**, 43-56.
- FLEET, M.E. (1975): The crystal structure of paratacamite, $\text{Cu}_2(\text{OH})_3\text{Cl}$. *Acta Crystallogr.* **B31**, 183-187.
- FLEISCHER, M. (1973): New mineral names. *Am. Mineral.* **58**, 560-562.
- FRONDEL, C. (1950): On paratacamite and some related copper chlorides. *Mineral. Mag.* **29**, 34-45.
- HANNINGTON, M.D. (1993): The formation of atacamite during weathering of sulfides on the modern seafloor. *Can. Mineral.* **31**, 945-956.
- HAWTHORNE, F.C. (1985): Refinement of the crystal structure of botallackite. *Mineral. Mag.* **49**, 87-89.
- KRACHER, A. & PERTLIK, F. (1983): Zinkreicher Paratacamit, $\text{Cu}_3\text{Zn}(\text{OH})_6\text{Cl}_2$, aus der Herminia Mine, Sierra Gorda, Chile. *Ann. Naturhist. Mus. Wien* **85/A**, 93-97.
- NICKEL, E.H., CLOUT, J.F.M. & GARTRELL, B.J. (1994): Secondary nickel minerals from Widgiemooltha, Western Australia. *Mineral. Rec.* **25**, 283-291, 302.
- & MANDARINO, J.A. (1987): Procedures involving the IMA Commission on New Minerals and Mineral Names, and guidelines on mineral nomenclature. *Can. Mineral.* **25**, 353-377.
- OSWALD, H.R. & GUENTER, J.R. (1971): Crystal data on paratacamite $\gamma\text{-Cu}_2(\text{OH})_3\text{Cl}$. *J. Appl. Crystallogr.* **4**, 530-531.
- PALACHE, C., BERMAN, H. & FRONDEL, C. (1951): *The System of Mineralogy 2*. John Wiley & Sons, New York, N.Y.
- POLLARD, A.M., THOMAS, R.G. & WILLIAMS, P.A. (1989): Synthesis and stabilities of the basic copper (II) chlorides atacamite, paratacamite and botallackite. *Mineral. Mag.* **53**, 557-563.
- PRING, A., SNOW, M.R. & TIEKINK, E.R.T. (1987): Paratacamite from South Australia. *Trans. Roy. Soc. South Aust.* **3**, 127-128.
- SHARKEY, J.B. & LEWIN, S.Z. (1971): Conditions governing the formation of atacamite and paratacamite. *Am. Mineral.* **56**, 179-192.
- SMITH, G.F.H. (1906): Paratacamite, a new oxychloride of copper. *Mineral. Mag.* **14**, 170-177.
- WALTER-LEVY, L. & GOREAUD, M. (1969): Sur la formation des chlorures basiques cuivriques en solution aqueuse de 25 à 200°C. *Bull. Soc. Chim. France* **1969**(8), 2623-2634.
- WELLS, A.F. (1949): The crystal structure of atacamite and the crystal chemistry of cupric compounds. *Acta Crystallogr.* **2**, 175-180.
- DE WOLFF, P.M. (1953): Crystal structure of $\text{Co}_2(\text{OH})_3\text{Cl}$. *Acta Crystallogr.* **6**, 359-360.
- WOODS, T.L. & GARRELS, R.M. (1986): Phase relations of some cupric hydroxy minerals. *Econ. Geol.* **81**, 1989-2007.

Received September 19, 1994, revised manuscript accepted August 7, 1995.